Energy 360 3 (2025) 100014

Contents lists available at ScienceDirect

Energy 360

journal homepage: www2.cloud.editorialmanager.com/engy/default2.aspx

Optimizing high performance biochar from sugarcane bagasse and corncob via vacuum pyrolysis

Nakum Divyangkumar *, N.L. Panwar

Department of Renewable Energy Engineering, Maharana Pratap University of Agriculture and Technology, Udaipur, Rajasthan 313001, India

ARTICLE INFO

Keywords:
Biochar
Slow pyrolysis
Vacuum pyrolysis
Sugarcane bagasse
Corn cob

ABSTRACT

Biochar, a carbon-rich material, is the key to enhancing soil health while combating climate change. This research explores the synthesis and optimization of biochar from sugarcane bagasse and corncob using a vacuum pyrolyzer, aiming to harness its possible potential applications for sustainable agricultural and environmental solutions. Biochar with porous structures has been created in a slow pyrolyzer at three temperature ranges. Every biochar specimen underwent standard surface and elemental characterization methods, including proximate analysis, elemental analysis, scanning electron microscopy (SEM), Brunauer–Emmett–Teller (BET), Powder X-ray diffraction (XRD), and thermogravimetric analysis. The pyrolysis temperature had a negative effect on biochar yield and reduced from 30.21 to 25.4 % and 34.59 to 24.28 as the pyrolysis temperature increased from 500 to 700 °C for corncob and sugarcane bagasse respectively. The biochar formations were discovered to possess a higher proportion of elemental carbon (90–91 %) compared to their original state (43.9–45.2 %). The biochars obtained from sugarcane bagasse exhibited a higher maximum surface area of 185.85 m^2/g in contrast to the biochars derived from corn cob, which had a surface area of 69.29 m^2/g at 600 ℃. The biochars consistently demonstrate heightened potency in comparison to their original form, as revealed by comparative characterizations. Using optimal response surface method, optimal conditions were identified.

1. Introduction

Agricultural waste management and soil degradation are pressing global issues with far-reaching environmental, economic, and social implications. According to the report by Kolawole et. al. in 2024, over 659 million tons of agricultural residues are generated annually (Kolawole et al., 2024), presenting both challenges and opportunities. Improper disposal of these residues often leads to environmental pollution, including air quality deterioration due to open burning and leachate contamination of water bodies. At the same time, soils worldwide face significant degradation, losing organic matter and structure due to intensive farming practices, erosion, and climate change impacts (Divyangkumar and Panwar, 2024). This dual challenge necessitates innovative approaches to valorize agricultural residues while improving soil health.

One promising solution lies in converting agricultural residues into biochar, a carbon-rich material produced through pyrolysis (Lanjekar et al., 2024). Biochar not only offers a sustainable waste management option but also provides numerous agronomic benefits, including enhancing soil fertility, sequestering carbon, and improving water retention (Gęca et al., 2023). Its porous structure, negative surface functional groups, and high carbon content make it resistant to microbial decomposition and improve crop nutrient use efficiency (Alkharabsheh et al., 2021). Because of its enormous surface area and porous nature, biochar retains water and nutrients in both the soil's surface and subsurface (Khalil et al., 2021). This is why the article published by Bayoka et al. in 2023 referred to biochar as black gold (Bayoka et al., 2023). Biochar is produced from various biomasses, such as wood chips, crop straws, coconut shells, poultry litter, algae, sewage sludge, bamboo, and sawdust. Initially used for agriculture to improve soil quality and fertility, biochar is now being used in various fields such as heavy metal remediation, global climate change mitigation, mine tailing, and environmental pollutant management (Zhang et al., 2018; Wang et al., 2017; Egene et al., 2018). Biochar's high alkalinity reduces soil acidity and forms a suitable habitat for soil microbes (Huang et al., 2023). It also has a higher propensity to absorb cations and anions from solution. The pyrolysis process of biochar production reduces greenhouse gas emissions, such as sulfur oxides, nitrogen oxides, particulate

* Corresponding author.
E-mail addresses: divyangnakumofficial@gmail.com (N. Divyangkumar), nlpanwar@gmail.com (N.L. Panwar).

https://doi.org/10.1016/j.energ.2025.100014
Received 28 November 2024; Received in revised form 27 January 2025; Accepted 28 January 2025
Available online 1 February 2025

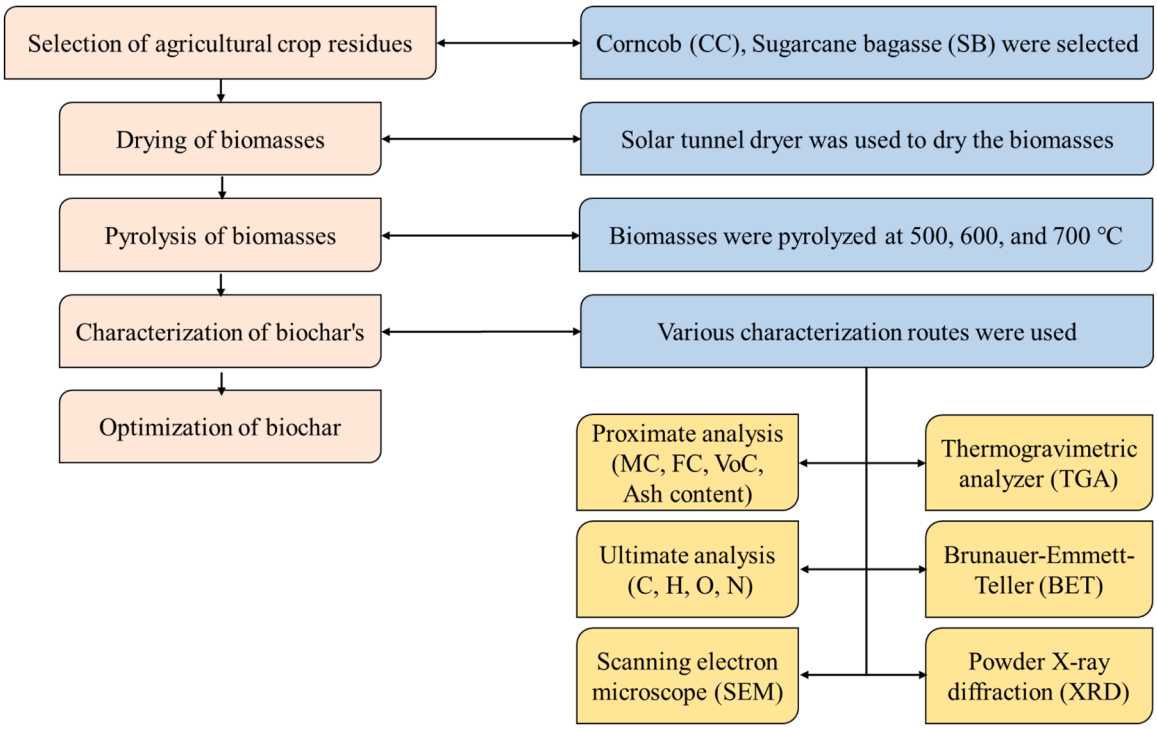

Fig. 1. The flow chart of biochar production and its characterization starting from selection of agricultural crop residues to optimization of biochar.

matter, and carbon dioxide (Dhar et al., 2022). The conversion of biomass into biochar helps remediate nature more effectively than conventional open incineration or dumping.

Among all the agricultural crop residues studied, sugarcane bagasse and corncob exhibit significant potential for biochar production. India produces 280 million tonnes of sugarcane bagasse and 22.23 million tonnes of corn cob (Roy et al., 2019). In the global list of maize-producing nations, India holds the 4th position in terms of area and the 7th position in terms of production, contributing approximately 4 % to the world's maize area and 2 % to the total production. In the fiscal year 2018–19, maize cultivation in India covered an area of 9.2 million hectares (El-Esawi, 2021). While India ranks second in sugarcane production after brazil (Mishra et al., 2021). At the end, substantial quantities of waste or byproducts are produced annually and incinerated in fields, leading to air, soil, and water contamination, and contributing to energy wastage (Kalair et al., 2021). By using a high-temperature carbonization method (100–800 °C), these agricultural waste materials could be repurposed to create biochar. The produced biochar can be used in number of ways for agriculture or commercial application to make the environment healthier. These approch should reflect increased awareness of environmental concerns and the importance of efficient waste management practices.

In this connection, the effort had been undertaken to produce the biochar from inexpensive agricultural waste products, such as sugarcane bagasse (SB) and corn cob (CC) using a vacuum pyrolyzer at three temperature ranges (500 to 700 ℃). In this study, vacuum pyrolysis was chosen due to its unique advantages over conventional pyrolysis. Operating under reduced pressure minimizes secondary reactions, such as tar re-polymerization, which can degrade biochar quality. This method enhances the yield and structural integrity of biochar by preserving its porous structure and functional groups, critical for applications like adsorption and soil amendment. Then, the physicochemical characteristics of biomass and produced biochar were determined to identify the potential suitability for possible applications by proximate analysis, ultimate analysis, SEM, BET, Powder XRD, and TGA. Lastly, the optimization using the optimal RSM model was done on the surface morphology of biochar.

2. Material and methods

This section covers the materials and methodology used for producing biochar and its characterization. The overall process flow chart for the study is presented in Fig. 1 below. The research work for producing and characterizing biochar was conducted at the Department of Renewable Energy Engineering, CTAE, Udaipur, India.

2.1. Biochar production

The sugarcane bagasse (SB) and corncob (CC) biomass were used for biochar production because of local availability and accessibility. The procured biomass generally contains high moisture content (MC) (above 10 %). The moisture content should be below 10 % for efficient pyrolysis of biomass (Eke et al., 2020). Thus, a drying process was followed to reduce the MC using the solar tunnel dryer available at DREE. The biomasses were placed in a solar dryer for 11 h on a sunny day. The proximate analysis was then done to identify the final moisture present in the biomass. The vacuum pyrolyzer machine (VPI) was used to produce biochar at three operating temperature ranges: 500 ℃, 600 ℃, and 700 ℃ with 2 hr residence time. A brief description and pictorial view of VPI is available in the previous research (Divyangkumar et al., 2024).

The yield of biochar, liquid oil, and noncondensable gas from SB and CC was calculated using the following equations.

$$Biochar\ yield(\%) = \frac{Biochar\ weight(Kg)}{Total\ feedstock\ weight(Kg)} \times 100$$

$$Liquid\ oil\ yield(\%) = \frac{Final\ liquid\ weight(Kg)}{Total\ feedstock\ weight(Kg)} \times 100$$

$$Gas\ yield(\%) = 100 - (Biochar\ yield + Liquid\ oil\ yield)$$

2.2. Characterization of produced biochar

The size of selected biomass and produced biochar was reduced using a grinder machine to accomplish the various characterization routes.

The proximate and ultimate analysis was done using ASTM standards. The proximate analysis of samples was done at the departmental laboratory. The proximate analysis measured the moisture content by ASTM E871–82, volatile content (ASTM E872–82), ash content (ASTM D1102–84), and fixed carbon evaluated by difference. The elemental analyzer was used for the ultimate analysis. The higher heating value (HHV) of biomass and all biochar were evaluated by the correlation model developed by (Nhuchhen and Abdul Salam, 2012). The thermogravimetric analysis (TGA) and differential thermogravimetric (DTG) of biomass and biochar were carried out at DREE itself. Whereas, scanning electron microscope (SEM), Brunauer Emmett teller (BET), and Powder X-ray diffraction (XRD) were done by outsourcing at Central Salt and Marine Research Institute (CSMCRI), Bhavnagar.

2.2.1. Scanning electron microscope (SEM) analysis

SEM examines and creates an image of the materials by using high-energy electron beams to scan the samples in different scan patterns and resolutions (Mujtaba et al., 2021). SEM analysis was performed on the chosen biomass, and biochar samples to find out more about their composition, topography, surface morphology, and other characteristics. The micrograph was taken at 500 magnifications. The SEM analysis was performed using a JEOlJSM 7100 F microscope at CSMCRI, Bhavnagar, Gujarat.

2.2.2. Brunauer emmett teller (BET) analysis

The BET analysis was also carried out at CSMCRI, Bhavnagar, Gujarat. Using N_2 sorption isotherms and a Brunauer-Emmett-Teller surface area analyzer, the total accessible surface area of the pyrolyzed biochars was calculated per unit mass (manufacturer: Micromeritics, model: ASAP 2010). The surface area (m^2/g), pore volume (cm^3/g), and pore size (nm) of raw biomass and produced biochar were measured by BET analysis. Initially, the selected samples were degassed by keeping the temperature between 200 and 250 °C in an inert atmosphere (with an N_2 environment) for two to four hours.

2.2.3. Powder x-ray diffraction (XRD)

The powder XRD technique is widely used to characterize or identify the crystallographic structure, physical properties, crystalline size, and chemical composition of solid samples (Stylianou et al., 2020). The Philips Xpert MPD instrument with Cu-Ka radiation located at CSMCRI, Bhavnagar, Gujarat was used to evaluate the P XRD of selected biomass and biochar samples. The P-XRD device is also utilized to estimate the crystallographic strain of the material. The chosen 2θ ranged from 5° to 80°.

2.2.4. Thermogravimetric analysis (TGA) and differential thermogravimetric (DTG)

The detailed study of all biomass and biochar samples was undertaken using TGA and DTG in an inert environment with a nitrogen flow rate of about 50 ml/min. The analysis was done in response to mass loss characteristics. The finely powdered sample weight (10 mg) was measured using the TGA analyzer (STA 7300 Hitachi, Germany) located in the departmental microbiology laboratory. The measurement involved a heating rate of 10 °C/min, starting from room temperature and reaching 1000 °C.

2.2.5. Optimization of biochar using RSM

The RSM is a well-known technique used in engineering applications to optimize process analysis. It uses statistical and mathematical methods to assess the possible impact of factorial factors on the outcome. Therefore, an RSM standard scheme was used to optimize every biochar. With the aid of ANOVA analysis, the response of every run was further taken into account for the optimal process parameters. The F-test is a crucial tool for assessing the overall effectiveness and influence of a model or the parameter under consideration in this regard.

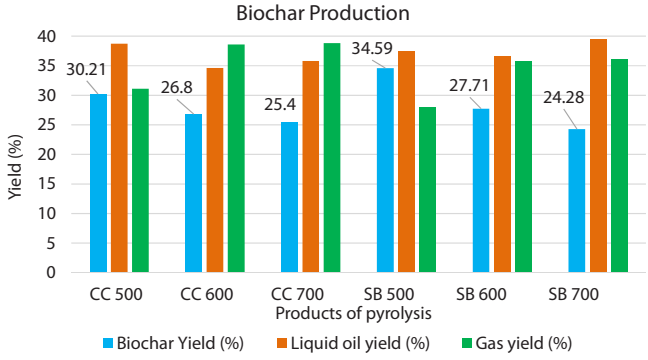

Fig. 2. Mass balance of pyrolysis products for CC and SB at 500 ℃, 600 ℃ and 700 ℃ temperatures. The biochar yield, liquid yield and gas yield of CC and SB biomass indicated with blue, orange and green color respectively.

3. Result and discussion

3.1. Biochar yield

A total six number of biochar were produced using SB and CC feedstock at three temperature ranges (500 ℃, 600 ℃, and 700 ℃) at 2 hr residence time. The biochar was allowed to cool until ambient temperature and then it was removed from the cartridge and weighed. The liquid accumulated at the bottom of the storage tank was extracted and weighed separately. The percentage value of each component was measured using the formula mentioned in the above section and the final gas yield was calculated by subtracting the biochar yield and liquid yield. The result indicated that the pyrolysis temperature significantly affects the biochar yield shown in Fig. 2. It was observed that the increased pyrolysis temperature resulted in decreasing biochar yield from 30 to 25% and 34 to 24% in CC and SB respectively. The biochar trend results are consistent with previously published research (Montero et al., 2018). However, the high temperature increased the pore opening in biochar, thus the quality of biochar was seen to improve at high pyrolysis temperatures. Additionally, the biochar yield in VPI is comparatively lower than atmospheric pyrolysis. This is due to the reduction in pressure and higher organic vapor removal rate, leading to a shortened residence time for the vapors and restricted secondary reactions (Foong et al., 2020).

3.2. Proximate and ultimate analysis

Proximate and ultimate analysis of biochar provide crucial insights into its suitability for improving soil health. The result of proximate analysis influence nutrient retention, pH adjustment, and soil structure improvement. While ultimate analysis reveals the understanding of biochar's nutrient content, stability, and potential environmental impacts.

The two biomass and six biochar samples produced at three different temperatures underwent proximate and ultimate analysis for identification of the moisture content (MC), volatile content (VC), ash content (AC), fixed carbon (FC), and elemental content, respectively. The obtained value of proximate and ultimate analysis is presented in Table 1. It was discovered that the moisture content of CC biochar and SB biochar slightly increased from 1.05 to 1.2% and 1.41 to 1.78% respectively. The increment of moisture content may be due to the openings of pores at elevated temperatures. Similar behavior was observed in fixed carbon and ash content. In the case of CC, the fixed carbon increased from 84.98% to 92.8%, and the ash content rose from 4.27% to 5.85%, while for SB biochar, the fixed carbon varied from 86.18% to 93.98% and the ash content from 3.83% to 4.05%. Whereas, the decreasing trend was found in volatile content and it was decreased from 9.69 to 0.15% and 5.58 to 0.19% in CC and SB biochar respectively. A similar trend of

Table 1
The Comparision of proximate, ultimate, and HHV analysis of biomass and biochar samples at 500 ℃, 600 ℃, and 700 ℃.

Samples	Proximate analysis (%)				Ultimate analysis (%)				HHV (MJ/kg)
	MC	VC	AC	FC	C	H	O	N	
CC	7.07	78.87	1.59	12.47	43.9	6.7	48.6	0.8	20.39
CC* (Gupta et al., 2018)	-	-	-	-	46.69	5.86	45.70	1.73	17.10
CC500	1.05	9.69	4.27	84.98	83.95	5.35	9.88	0.82	32.14
CC600	1.15	1.38	5.44	92.03	87.9	3.5	7.7	0.9	33.25
CC600* (Gupta et al., 2018)	-	-	-	-	80.22	3.87	14.84	1.05	19.97
CC700	1.2	0.15	5.85	92.8	90.6	2.7	5.6	1.1	33.33
SB	9.64	82.93	1.54	5.88	45.2	6.6	47.7	0.5	19.66
SB* (Sohaib et al., 2017)	6.21	82.38	2.94	8.47	45.39	7.92	46.67	0.15	-
SB500	1.41	8.58	3.83	86.18	81.77	4.52	12.78	0.93	32.49
SB600	1.69	0.95	3.98	93.38	85.51	3.88	9.52	1.09	33.84
SB600* (Sohaib et al., 2017)	2.97	20.35	7.58	69.10	66.38	4.62	28.52	0.48	-
SB700	1.78	0.19	4.05	93.98	91.51	3.11	3.97	1.41	33.96

* The relevant data compared with previous study

Table 2
The results of BET analysis for biomass and biochar samples derived at 500 ℃, 600 ℃, and 700 ℃.

Sample Name	Surface area (m^2/g)	Pore volume (cm^3/g)
CC	1.2541 ± 0.0138	0.003366
CC500	1.6997 ± 0.0063	0.003888
CC600	69.2998 ± 3.3770	0.012234
CC600* (Gupta et al., 2018)	30.98	-
CC700	3.4208 ± 0.0182	0.005659
SB	2.0800 ± 0.0465	0.003676
SB500	60.1537 ± 3.5433	0.004563
SB600	185.8569 ± 2.4542	0.057261
SB600* (Inyang et al., 2010)	14.07	-
SB700	7.3261 ± 0.0959	0.006179

* The data obtained and compared with previous study

proximate analysis was found by (Divyangkumar et al., 2024; Durango Padilla et al., 2024). It is also seen from Table 1 that; a higher amount of fixed carbon content was found in all biochar at various temperatures compared to their raw feedstock. Almost, 6 to 7 times and 14 to 16 times increment in fixed carbon content was observed in CC and SB biochar when compared to their raw biomass. These results demonstrated that converting biomass to biochar produced beneficial results because high-fixed-carbon biochar has more potential for use as a soil supplement to absorb carbon and mitigate climate change. Compared to the raw biomass of CC and SB, the biochar contains a lower percentage of volatile matter and high ash content, indicating that the removal of oxygen-based chemical groups leads to mineral accumulation during the thermochemical conversion of organic waste.

A significant change was observed in carbon content as the pyrolysis temperature increased from 500 to 700 ℃. It was observed that the carbon content varied from 83.95 to 90.6% and 81.77 to 93.98% in CC and SB-derived biochar respectively. On the other hand, in CC biochar, the hydrogen and oxygen levels dramatically dropped from 5.35% to 2.7% and 9.88% to 5.66%, respectively, as the pyrolysis temperature increased. Similarly in SB biochar it droped from 4.52% to 3.11% and 12.78 to 3.97% respectively. The minimum amount of nitrogen content was found in all biomass and biochar samples. However, the inorganic mineral nitrogen content increased slightly with temperature because of the removal of organic volatile content. These findings are aligned with earlier research (de Almeida et al., 2022; Toscano Miranda et al., 2021; Adekanye et al., 2022). The highest temperature caused the biomass to completely decompose thermally, producing highly carbonaceous biochar. During the pyrolysis of biomass, increasing the degree of polymerization led to a more compact carbon structure and an increase in the carbon content of biochar (Domingues et al., 2017).

The heating value of a substance is mostly dependent on its carbon content. The resulting biochar exhibited a higher heating value when compared to biomass (Liu et al., 2019). The estimated heating values of CC biochar generated at 500, 600, and 700 °C were 32.14, 33.25, and 33.33 MJ/kg, respectively; these values were greater than the raw CC biomass (20.39 MJ/kg). on the other hand, the heating values of SB biochar varied from 32.49 to 33.96 MJ/kg compared to 19.66 MJ/kg for raw SB biomass. The obtained result of HHV of all biochar is comparable to coal having a 30 MJ/kg (Qian et al., 2020). Table 1 also compared the findings of the study with previous literature to indicate the novelty of the results by vacuum pyrolysis.

3.3. Brunauer emmett teller analysis

A higher surface area enhances biochar's ability to adsorb nutrients, reduce leaching, and improve soil fertility. The porous structure promotes better aeration and water retention, supporting microbial activity and plant growth, thereby contributing to improved soil health. Table 2 represents the specific surface area of biomass and biochar samples produced at different temperatures. The increasing trend of specific surface area was observed from biomass to biochar formation with temperatures.

The BET analysis showed that the raw CC and SB had surface area and pore volume of 1.25, 2.08 m^2/g and 0.012234, 0.003676 cm^3/g, respectively. As the temperature for pyrolysis increased from 500 to 600 ℃, the specific surface area increased from 1.69 to 69.29 for CC and 60.15 to 185.85 for SB biochar respectively. Similarly, pore volume is also increased. The study discovered that the surface area and pore volume of the biochar samples increased dramatically when the pyrolysis temperature rose to 600 ℃. This resulted from the elimination of volatile components during the pyrolysis of biomass, specifically the volatilization of organic molecules, which left voids in the structure of the biochar (Liew et al., 2018). Large surface areas are created in biochar produced by vacuum pyrolysis because of the opening of pores throughout the process caused by the acceleration of devolatilization during the vacuum production process, which lowers product partial pressure and gas retention time (Uras et al., 2012). Additionally, when pyrolysis temperature rises, pore-blocking within the structure is pushed out or thermally destroyed, increasing the biochar's surface area. Following the full breakdown of the amorphous hemicelluloses, cellulose was primarily responsible for increasing the surface area in this temperature range (Dhar et al., 2022). After the breakdown of glycosidic chains, cellulose microfibrils generated graphitic layers, which regulated the dimensional changes (Jindo et al., 2014). Similar findings of biochar derived from different types of biomasses have been reported by a number of researchers (Smith and Rodrigues, 2015; Wang et al., 2022). Because vacuum pyrolysis can remove volatile matter quickly, reduce secondary reactions, and enhance the porosity and surface area of biochar, it is recommended over atmospheric pyrolysis (Nam et al., 2018).

In contrast, the reduction of surface area was observed at the further increase in pyrolysis temperature from 600 to 700 ℃. The blockage of

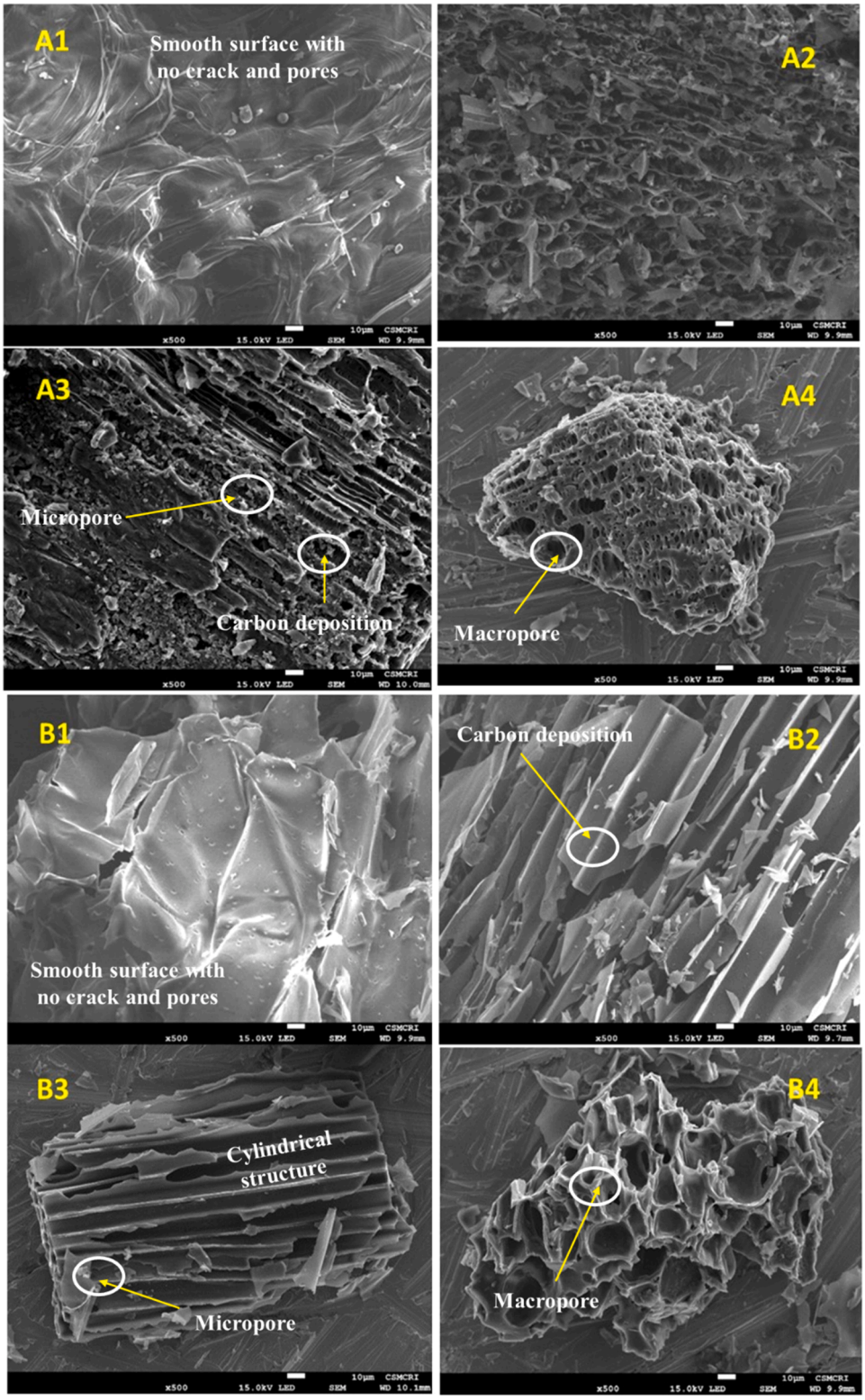

Fig. 3. SEM images of CC biomass **(A1)**, CC 500 **(A2)**, CC 600 **(A3)**, CC 700 **(A4)**, SB biomass **(B1)**, SB 500 **(B2)**, SB 600 **(B3)**, and SB 700 **(B4)**. The figure demonstrated the changes in surface morphology in biochar with rising temperature.

pores by inorganic ash compounds was the reason for this phenomenon. The same things can be observed through SEM analysis (refer Fig. 3). Furthermore, the disintegrated and amorphous products of additional condensed volatiles were responsible (Dhar et al., 2022). According to research by (Ronsse et al., 2013)., the specific surface area of the biochars decreased as the number of inorganic components rose. Molten ash has the potential to penetrate the pores of the biochars that are generated (Ronsse et al., 2013). Every sample of biochar exhibited both macro and microporous structures. Because of its microporous structure, biochar is a great adsorbent for treating water, wastewater, and air (David, 2022). According to (Nair et al., 2017)., the soil treated with biochar had increased pore volume and water absorption capacity due to

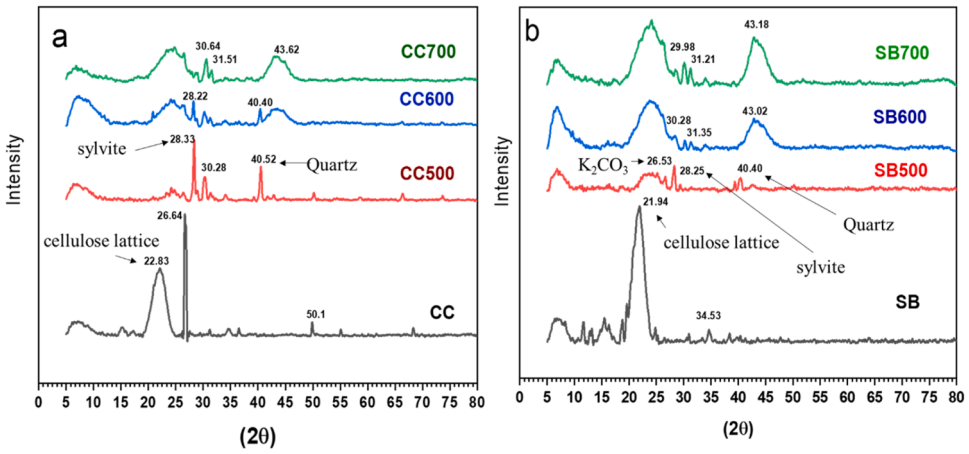

Fig. 4. **4a**: Representation of the XRD spectra of CC biomass and their derived biochar at at 500 ℃, 600 ℃, and 700 ℃. **4b**: Representation of the XRD spectra of SB biomass and their derived biochar at at 500 ℃, 600 ℃, and 700 ℃. The figure indicating different phases elements presents in biomasses and all biochar samples.

the increase in pyrolysis temperature. According to (Lei and Zhang, 2013), the specific surface area of woody biochar treated at high temperatures increased by up to 8–12 times, suggesting that they might be useful for the humification of sandy soil. According to research by (Liang et al., 2006)., adding biochar to anthrasols increased the soil's surface area by up to 4.8 times. Additionally, a high surface area is beneficial for developing polymeric biocomposites, which is now an emerging and novel application in replacing conventional harmful compounds.

3.4. Scanning electron microscope analysis

The SEM analysis revealed the surface morphology of biomass and biochar. The result of SEM analysis is presented in Fig. 3. Using SEM images, surface morphological differences and structural modifications of the biochars were examined in terms of porosity. This analysis is crucial for soil health as they influence biochar's ability to improve soil aeration, water retention, and nutrient adsorption. SEM can reveal biochar's pore structure, which facilitates microbial habitat and enhances cation exchange capacity, contributing to better nutrient cycling and soil fertility.

The figure showed that the biochar had a porous structure that was determined by SEM at temperatures between 500 and 700 °C at a resolution of 500. There are differences in these porous formations. The CC biomass (A1) and SB biomass (B1) contained smooth surfaces with no cracks, pores, or crevices and a non-porous, showing plain morphology. During the thermal treatments of biomass, as the pyrolysis temperature increases, the more volatile matter is released from the biomass, resulting in more porous structures on the surface (Tomczyk et al., 2020). The uneven surface structure of resultant biochar would be due to the shrinkages of biomass particles during the pyrolysis process (Chen et al., 2018). The shrinkage was observed in coconut fiber biochar by (Dhar et al., 2022). There were various macropore, micropore, and mesopore shapes and sizes seen throughout the pictures. Upon subjecting the biochar to defined pyrolysis conditions, a distinct pattern emerged across all samples, revealing a honeycomb-like network adorning their surfaces. This distinctive feature was accompanied by the presence of well-developed macropores, underscoring the unique structural characteristics induced by the specific pyrolysis conditions applied.

In comparison to the raw biomass, the biochar has a far more spectacular surface appearance since the greater pyrolysis temperature completely degraded the cellulose, hemicellulose, and lignin. According to (Gao et al., 2013) the biochars that underwent greater temperature pyrolyzation had a comparatively larger surface area. The particles of the SB biochar retain some original shapes after carbonization and smash because of their higher content of lignocellulose (Qiu et al., 2019). The pyrolysis process produced well-defined hollow carbon channel arrays, indicating the production of CC biochar through biomass pyrolysis (Assirey and Altamimi, 2021). The cylindrical, rough, uneven, and porous structure of the biochar generated from SB was visible in the SEM micrographs (Tehreem et al., 2022). SB biochar (B3, B4) showed a cylindrical porous structure at 500 magnifications. Additionally, the white deposits were seen as a result of the carbon content deposition. The tiny circular bodies were visible on the CC biochar (A2) surface at 500 magnifications, according to research performed by (Tehreem et al., 2022). However, the SB biochar exhibited a comparatively high porous structure than CC biochar in all temperature ranges as observed in Fig. 3. Additionally, A4 and B4 biochar sample indicated reduced porosity because of molten ash infiltration in the pores, that validate the outcomes of BET analysis in Section 3.3. This result suggests that during the pyrolysis treatment, the biomass selection had a significant impact on how the morphological features evolved.

The high quality of biochar can be used for many applications for environment remediation. Liu et al. discovered that the intra-pores generated within the biochars boosted the capacity to retain water in sandy soil (Liu et al., 2017). Biochars with porous structures offer ideal living spaces for soil microorganisms such as fungi, algae, and actinomycetes. These microorganisms provide a source of food for soil biota and soil animals (Briones, 2014). These microbial communities are preserved and increased when porous biochar is added to the soil.

3.5. Powder x-ray diffraction

This analysis reveals the biochar's mineral composition, including essential nutrients and trace elements, which influence its ability to improve soil fertility. The primary components of biomass are polymeric crystallographic structures such as cellulose, hemicelluloses, and lignin. This structure is distinct from the amorphous structure of other materials (Değermenci et al., 2019). Fig. 4a and b represent the XRD spectra of biomass and biochar for CC and SB respectively.

The XRD diffractogram is presented in Fig. 4, where a large peak at 2θ values approximately around 22.83° and 21.94° are seen in CC and SB respectively. This peak indicates the crystalline nature of the cellulose lattice spacings within biomass (Nazir et al., 2022). As the pyrolysis temperature rises for the specific biochar samples, the crystalline cellulose peak vanishes. The findings suggest that the crystal structure underwent disruption as a result of the complete thermal breakdown of biomass at a different temperature range. As a result, amorphous biochar rich in carbon was formed. Stable carbonaceous material is also indicated by broad peaks. A similar result in CC biochar was found by (Pinky et al., 2023). The lack of any distinct peaks, however, suggested that there was no crystallinity, which could have resulted from the

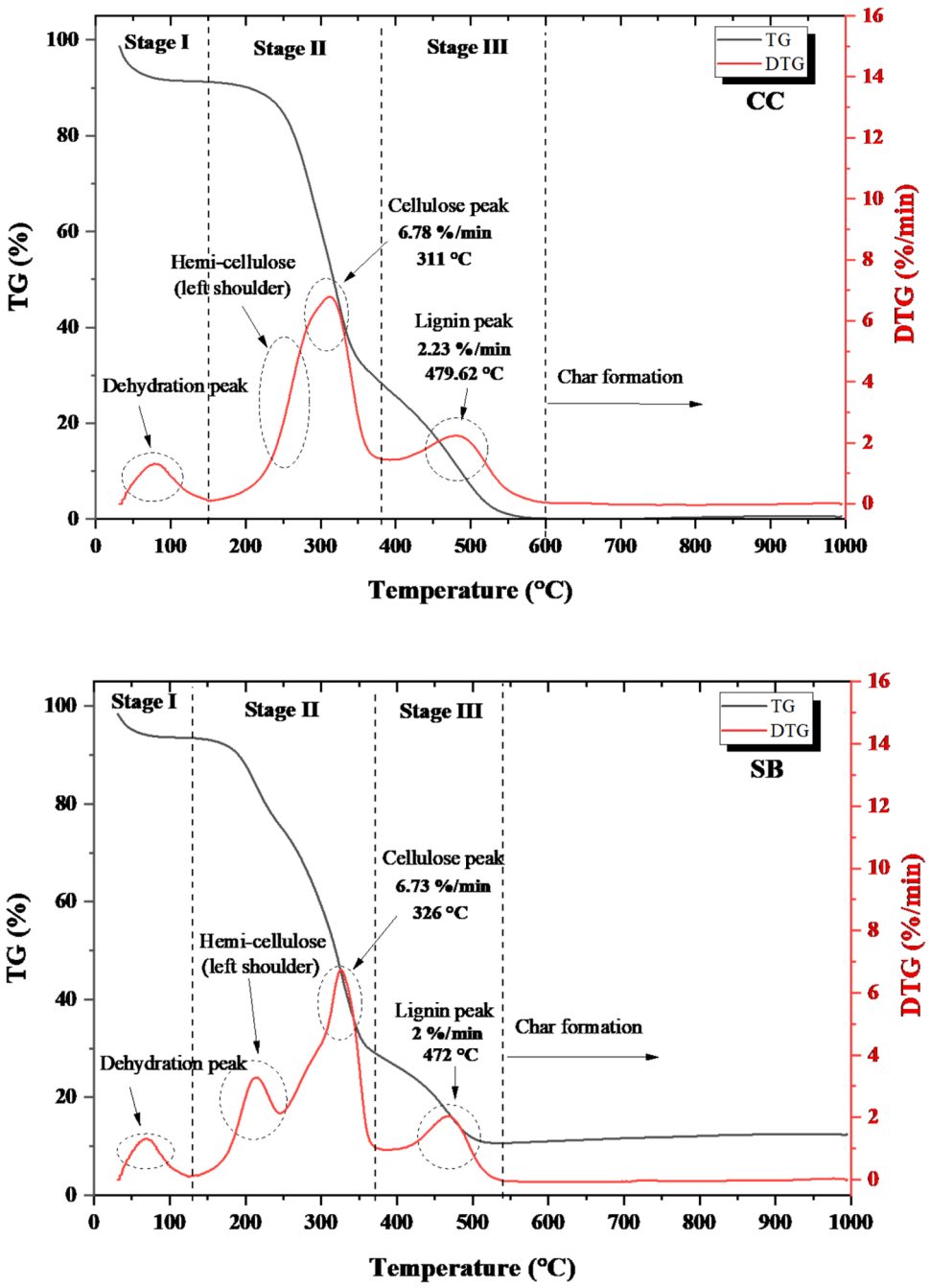

Fig. 5a. TG-DTG characteristics of CC and SB biomass at 10 °C/min.

existence of silica or other pertinent inorganic metal oxide impurities (Mohan et al., 2018). There is a difference between the biochars' peak intensity and peak structure. Both the crystal size and crystallinity have an impact on them (Bourke et al., 2007). Smaller crystal sizes are represented by wider diffraction peaks. Analyzing the diffraction peaks in the biochar suggests that the SB biochar likely consists of graphite and amorphous carbon, exhibiting smaller sizes than the other. A minor diffraction peak indicative of K_2CO_3 is identified in the SB biochar at 2θ of approx 26^0 (Qiu et al., 2019). The spike observed at 2θ of 28.33°and 28.25° in the XRD pattern of the CC and SB biochar respectively indicates the existence of sylvite. Quartz (SiO_2) may be detected in all biochar samples by looking for the peak at 2θ = 40.52° and 40.40° for CC and SB biochar respectively. All biochar contains calcite, which has a limited peak height at 2θ of 50 to 51° ($CaCO_3$). Hence, the existence of calcite in biochar suggests elevated alkalinity in the specific biochar. The peaks of crystalline substances are well-defined, while the peaks of non-crystalline or amorphous substances are hollow.

3.6. Thermo gravimetric and derivative thermal gravimetry analysis of biomass and biochar

These analyses of biochar provide insights into its thermal stability, decomposition patterns, and organic and inorganic composition. The TGA findings at a rate of 10 °C/min of biomass and biochar samples are displayed in Figs. 5a and 5b. The experiment was conducted at the ambient temperature to 800 °C.

In the case of CC biomass, Fig. 5a shows the temperature ranges from 35 to 150 °C in the first stage, known as the dehydration stage, with an 7–8% mass loss. From 35 to 75 °C, unbound moisture is released, and from 75 to 150 °C, extractives and bound moisture are removed. The

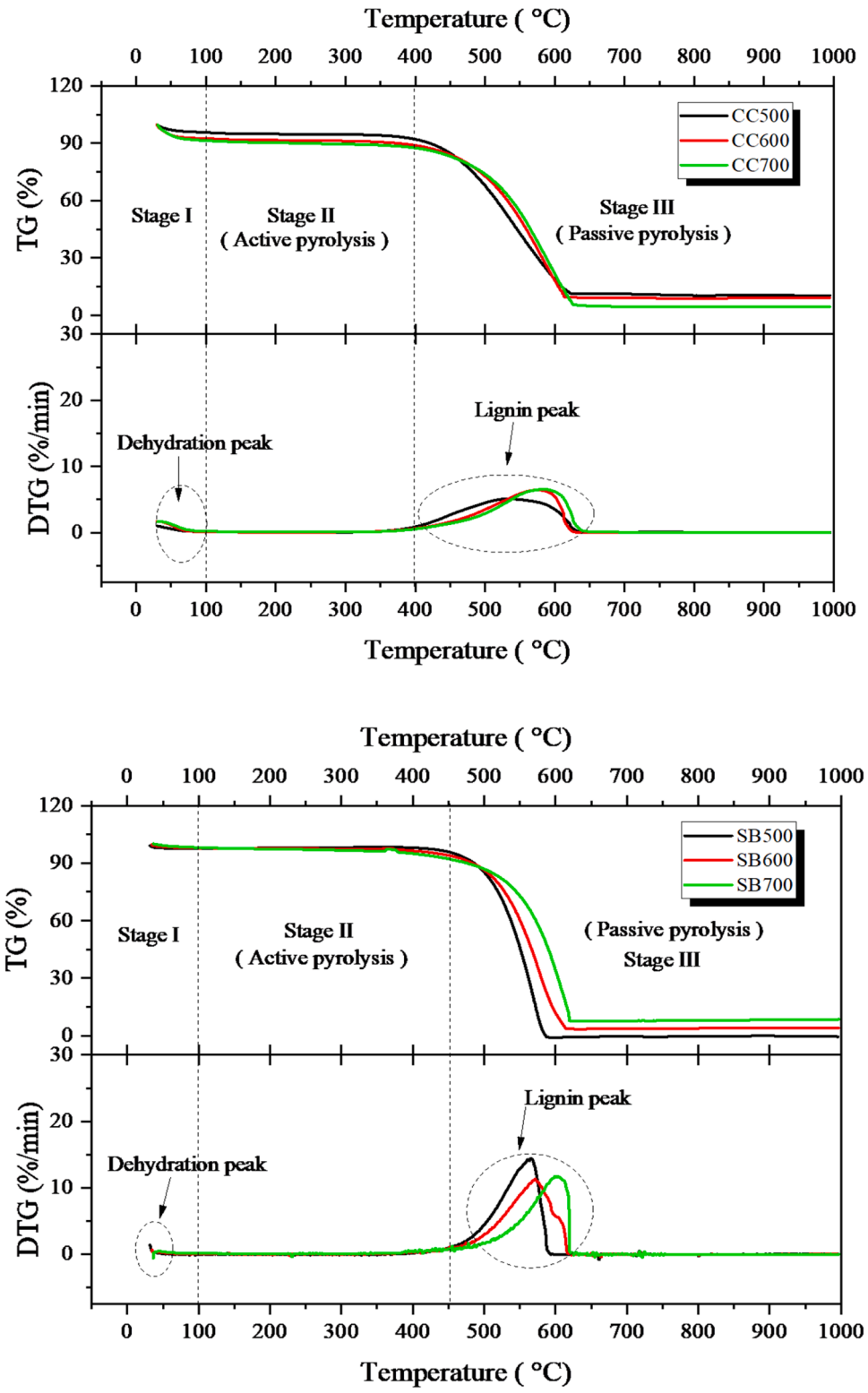

Fig. 5b. TG-DTG characteristics at 10 °C/min of CC and SB biochar samples derived at 500 °C, 600 °C, and 700 °C.

second stage, the active pyrolysis phase, occurs between 150 and 380 °C, where 62.5% mass loss happens due to the decomposition of volatile components, including hemicellulose and cellulose, similar to findings by (Padilla et al., 2019). The third stage, from 380 to 600 °C, involves lignin decomposition, leading to a 20% mass loss. This stage features overlapping exothermic and endothermic reactions. Finally, between 600 and 1000 °C, mass loss stabilizes, indicating complete conversion of biomass to char. Similarly, in SB biomass a small mass loss (4–5%) occurs up to 130 °C due to moisture evaporation. In the active pyrolysis zone (130–370 °C), hemicellulose and cellulose degrade, leading to a significant mass loss of 63%. Lignin degradation starts between 370–540 °C, resulting in an additional 16–18% mass loss. Beyond 540 °C, constant mass loss continues up to 1000 °C, indicating the complete conversion of SB biomass into char. The thermal behavior of

Table 3
Analysis of variance (ANOVA) of the Quartic model for surface morphology of all biochar samples derived from CC and SB biomass at 500 ℃, 600 ℃, and 700 ℃ temperature.

Source	Sum of squares	df	Mean square	F-value	p-value	
Model	182.63	8	22.83	3737.05	0.0003	significant
A-Temperature	0.5354	1	0.5354	87.65	0.0112	
B-Biomass	20.91	1	20.91	3422.82	0.0003	
AB	0.1448	1	0.1448	23.71	0.0397	
A^2	9.55	1	9.55	1563.05	0.0006	
A^2B	0.0002	1	0.0002	0.0310	0.8765	
A^3	0.0669	1	0.0669	10.95	0.0805	
A^3B	0.2930	1	0.2930	47.96	0.0202	
A^4	1.15	1	1.15	188.53	0.0053	
Residual	0.0122	2	0.0061			
Lack of Fit	0.0121	1	0.0121	92.66	0.0659	not significant
Pure Error	0.0001	1	0.0001			
Cor Total	182.64	10				

SB biomass was in good agreement with a previous study by (El-Sayed and Mostafa, 2015).

The thermal degradation curve of CC and SB biochar at a heating rate of 10 °C/min is presented in Fig. 5b. In CC biochar, moisture was released from the biochar, causing a slight curve up to 100 °C (Fig. 5b). About 1–3% moisture was released before 100 °C, indicating the biochar regained moisture from the atmosphere. Starting from 400 °C, a rapid decrease in weight due to carbon oxidation ends at 615 °C for the CC biochars, with weight losses of 77–80%, representing the effective carbon (Qiu et al., 2019). The thermal profile of CC biochar shows the peak between 100 to 400 °C in CC biomass (Fig. 5a) has disappeared. The biochar samples showed minimal mass loss, indicating high thermal stability. No mass loss was observed above 650 °C, showing that the pyrolysis process had little impact on the physicochemical characteristics of biochar over time (Sun et al., 2017). Biswas et al. in 2017 noted a similar pattern in their TG-DTG study of corncob biochar (Biswas et al., 2017). The TG and DTG curves for all biochars show a similar pattern. In SB biochar, minor left shoulder below 100 °C indicates moisture release. The SB biomass displayed thermal degradation peaks between 150 °C and 400 °C, which were absent in the biochar's TGA graph. The TG and DTG curves showed a minimal mass loss of about 14% up to 500 °C, suggesting exceptional thermal stability. In the biochar, thermal degradation started at 450 °C and ended at 630 °C, with an 87% mass loss. Beyond 630 °C, no significant mass loss was observed, indicating that extending pyrolysis time has minimal impact on biochar properties.

3.7. Statistical analysis

This study conducted through eleven distinct experimental runs, utilizing a combination of parameter configurations recommended by the CCD of the RSM approach, implemented via Design Expert-13 software. RSM provides an effective approach for optimizing process parameters by systematically analyzing the interactions and relationships among multiple variables. It minimizes the need for experimental trials, determines optimal conditions, and offers a thorough insight into interactions, enhancing process performance and system efficiency (Patel and Panwar, 2024). In the optimization process analysis, the reaction temperature (parameter A) and biomass type (parameter B) were noted as the important process factors and response variable was the surface area. Additionally, Table 3 mentions the results of the ANOVA. The quadratic model was recommended by Design Expert software for the optimization process across all responses, and it was deemed suitable for this study. The model also generated the coefficient values of R^2, F, and P values. The acceptability and relevance of the quadratic model are primarily determined by its F-value and P-value. The significant impacts of each run are represented by all these values.

A well-known technique for comparing the created model with the response data is regression model analysis (Siddiqui et al., 2019). Using high F test values and low P values to compare the mean squares of the regressed model with residuals (the probability for noise) is a crucial step in the process. Regression models that are reliable and consistent should exhibit a high F-value. A more accurate and efficient model is indicated by high F test values with low P values (Mubarak et al., 2011). The experimental study yielded a value of F of 3737.05 and a reduced P value (< 0.0001) for the constructed model, indicating the model's effectiveness and utility. The applicability of the regression model is primarily assessed through the "Lack of Fit" value in the ANOVA table. The insignificance of the "Lack of Fit" statistic indicates the model's accuracy and reliability (Arafat Hossain et al., 2017). The regression coefficient (R^2) was utilized to determine the regression model that most accurately represents the experimental data (Jawad et al., 2021). R^2 was computed to assess the regression equation's fitness. R^2 values vary from 0 to 1, with 0 representing a lack of fitness and 1 representing a highly perfect model (Abnisa et al., 2011). According to this study, the model's importance is demonstrated by the reasonably close coefficient of determination ($R^2 = 0.9999$) and adjusted coefficient of determination (R^2 adj = 0.9997). The proximity of these values to 1 indicates that the generated models exhibit a high degree of precision and accuracy.

The model equation that was created for change in surface morphology was as follows. The surface area of the created biochar served as the output response in the equation with temperature denoted by symbol A. Synergistic effects are shown by the positive sign, while antagonistic effects are indicated by the negative sign. Values of F, show how significantly different variables affect surface morphology.

$$SB = 6540{\cdot}50208 - 44{\cdot}41A + 0{\cdot}1112A^2\text{-}0{\cdot}000124A^3 + 5{\cdot}081{*}10^{-08}A^4$$

$$CC = 5968{\cdot}7088 - 41{\cdot}55A + 0{\cdot}107150A^2\text{-}0{\cdot}000121A^3 + 5{\cdot}081{*}10^{-08}\,A^4$$

The results of the ANOVA study indicated that temperature (A) had a less significant effect on the surface area (F values 87.65), while biomass (B) was determined to be the most significant variable with the greatest F-value of 3422.82 for the larger surface area. The biochar production process was optimized to achieve the maximum possible surface area, which resulted in a surface area of 186.839 m^2/g at an optimal temperature of 595 ℃ with a desirability value of 1, as shown in Fig. 6a. This predicted value was found to be in close agreement with the experimental findings, where the highest observed surface area was 185.85 m^2/g at a slightly higher temperature of 600 ℃. To evaluate the reliability and robustness of the optimization process, the reaction was analyzed by graphing it in relation to variations caused by noise. This analysis involved selecting a reference point and fine-tuning specific ranges to explore and identify the ideal correlation between the actual experimental values and any deviations resulting from noise. A detailed comparison between the predicted values and the actual experimental product yields is presented in Fig. 6b. The comparison underscores the strong agreement between the predicted and experimental results, demonstrating the accuracy and reliability of the model. This close alignment of values confirms the model's suitability and indicates that

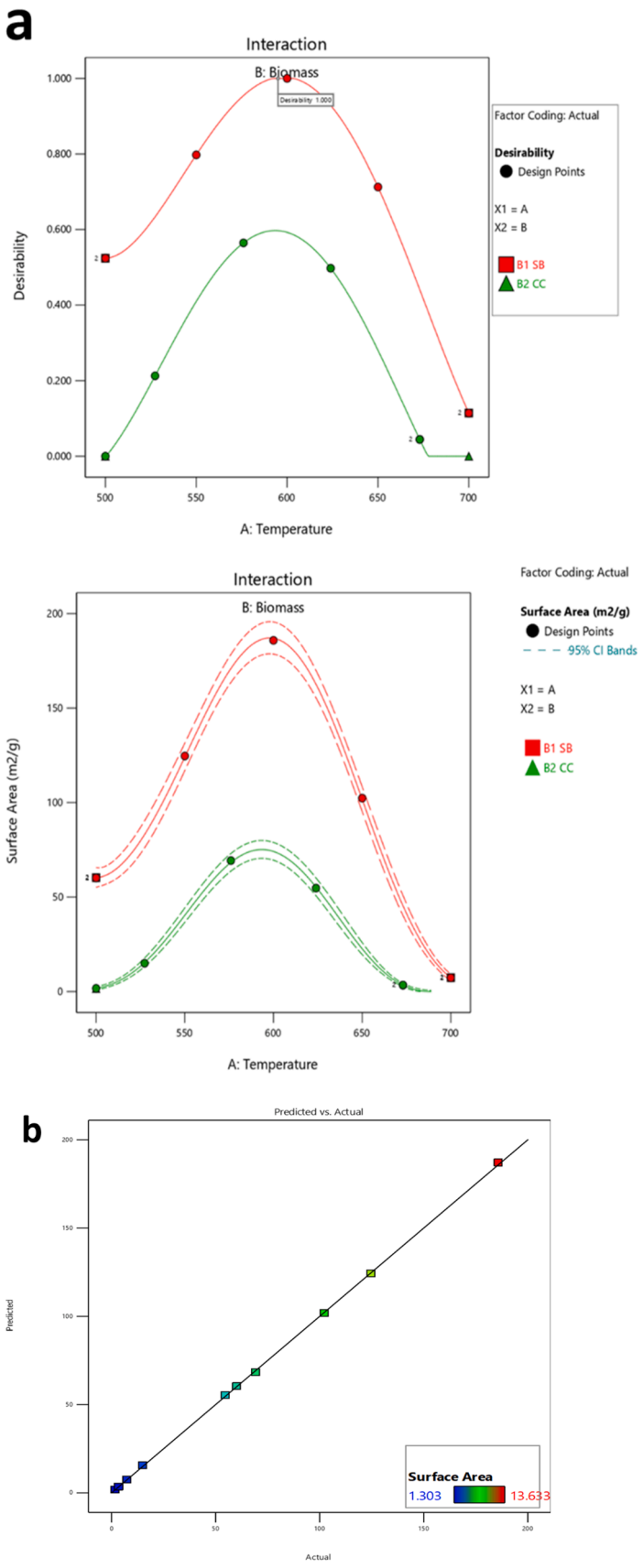

Fig. 6. (a, b): 4a: interaction between temperature and surface area, temperature and desirability, 4b: Relationship between predicted and actual values of surface area.

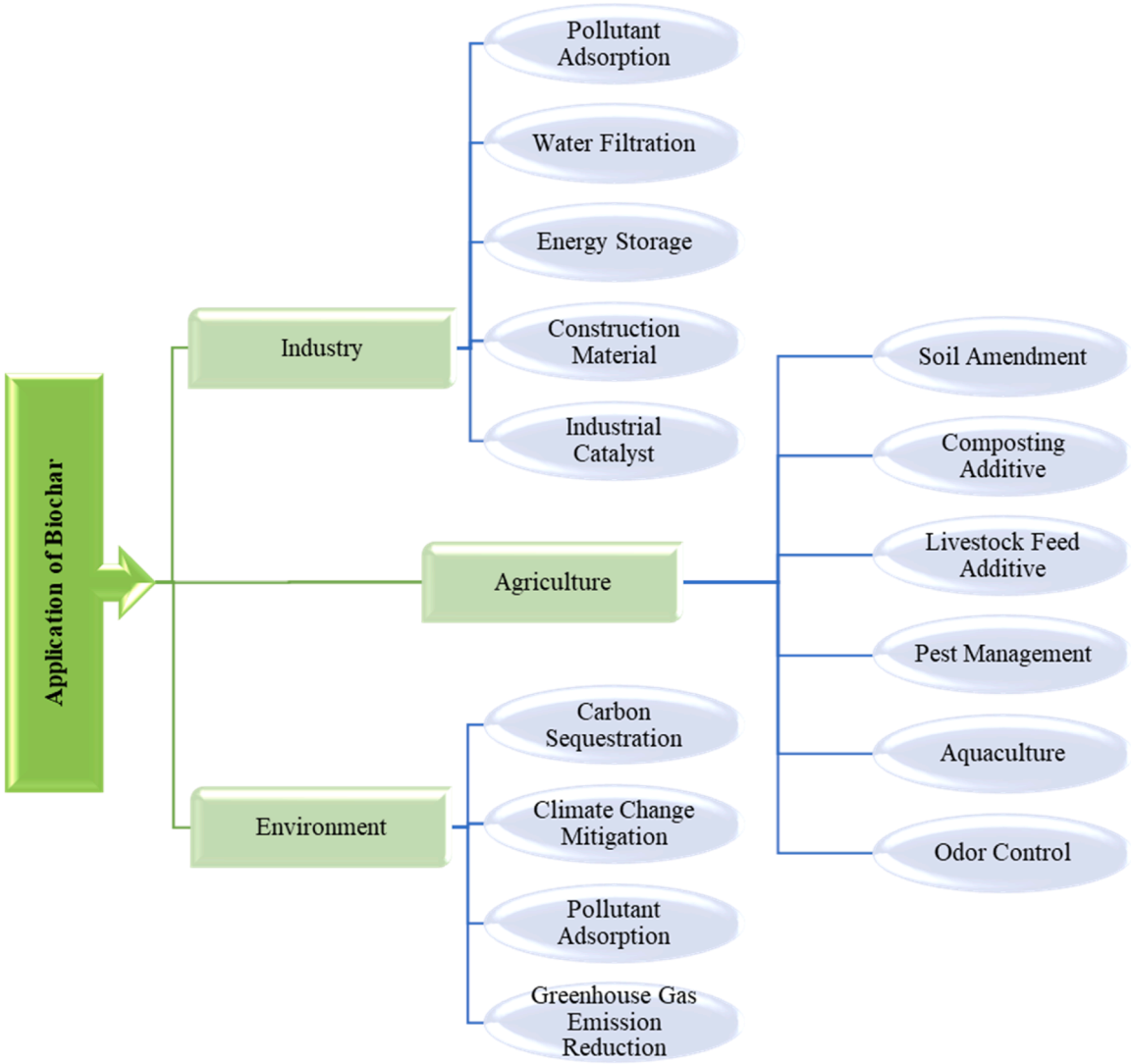

Fig. 7. The various applications of biochar in terms of industry, agriculture and environmental aspect.

the influence of noise on the results was minimal, thereby validating the optimization approach.

4. Environmental and economic aspect of biochar

The biochar derived from sugarcane bagasse and corncob using a vacuum pyrolyzer presents significant potential for addressing global challenges such as climate change and sustainable economic development. Its high carbon sequestration capacity can contribute to reducing atmospheric CO_2 levels, thereby aiding climate change mitigation. Furthermore, its use as a soil amendment enhances soil fertility and agricultural productivity, potentially reducing the need for synthetic fertilizers and their associated environmental footprint. The previous article (Divyangkumar et al., 2024) reported that, the applying biochar to soil for carbon sequestration can reduce GWP. Economically, this biochar valorizes agricultural residues, providing a cost-effective and sustainable solution for waste management while fostering circular economy practices. The detailed environmental and economic impact caused by production of biochar are discussed in previous research (Divyangkumar et al., 2024).

5. Application of biochar

The synthesized biochar exhibits properties that hold significant potential for various real-world applications (Fig. 7). For instance, biochar's high carbon content and stability make it an excellent candidate for carbon sequestration, aiding in mitigating greenhouse gas emissions by locking carbon in the soil for extended periods (V and Panwar, 2024). Additionally, its porous structure and nutrient-retention capacity enhance its effectiveness as a soil amendment, improving soil fertility, water retention, and crop productivity. Furthermore, due to its high surface area and adsorption capacity, biochar can serve as an efficient material for pollutant adsorption, effectively removing heavy metals, organic pollutants, and other contaminants from water and soil systems. These applications underline the environmental and agricultural relevance of biochar, adding practical value to the findings presented in this study.

6. Conclusion

This study advances biochar production techniques by employing a vacuum pyrolyzer, which enhances yield efficiency and optimizes key properties. The results showed that the production of biochar and volatile matter declined as the pyrolysis temperature increased. Nevertheless, the pyrolysis temperature elevation led to an increase in fixed carbon and ash content, BET surface area, degree of aromaticity, and porosity for all biochars. The optimization results revealed that the biomass and temperature significantly impact the surface area of

biochar. The optimized biochar was obtained at 595 ℃ with the highest surface area of 186.84 m^2/g. These qualities contribute to classifying biochars as a potent component for carbon sequestration, preserving nutrients and water in the soil, and unleashing numerous potential applications in both commercial and agricultural contexts. Future research should explore scaling up vacuum pyrolysis technology, assessing long-term impacts of biochar in diverse soil types, and integrating biochar usage into climate change mitigation policies to broaden its practical and global relevance.

Ethical approval and consent to participate

This work does not contain any studies with human participants or animals. All authors provided informed consent to participate in this study.

Supplementary information

The online version does not contain supplementary material.

Funding

Not applicable to this study.

CRediT authorship contribution statement

Nakum Divyangkumar: Conceptualization, Data curation, and writing the original draft; **N. L. Panwar:** Supervision, Writing - Reviewing and Editing.

Declaration of Competing Interest

The authors declare that they have no known competing financial interests or personal relationships that could have appeared to influence the work reported in this paper.

Acknowledgements

The authors are grateful to Department of Renewable Energy Engineering, Maharana Pratap University of Agriculture and Technology for providing the required facilities to conduct research successfully. The authors are also grateful to the Indian Council of Agricultural Research, Govt. of India, for providing financial aid to complete the research project under the Consortium Research Platform on Energy from Agriculture.

Data availability

No data was used for the research described in the article.

References

Abnisa, F., Wan Daud, W.M.A., Sahu, J.N., 2011. Optimization and characterization studies on bio-oil production from palm shell by pyrolysis using response surface methodology. Biomass-.-. Bioenergy 35, 3604–3616. https://doi.org/10.1016/j.biombioe.2011.05.011.

Adekanye, T., Dada, O., Kolapo, J., 2022. Pyrolysis of maize cob at different temperatures for biochar production: proximate, ultimate and spectroscopic characterisation. Res. Agric. Eng. 68, 27–34. https://doi.org/10.17221/106/2020-RAE.

Alkharabsheh, H.M., Seleiman, M.F., Battaglia, M.L., Shami, A., Jalal, R.S., Alhammad, B. A., et al., 2021. Biochar and its broad impacts in soil quality and fertility, nutrient leaching and crop productivity: a review. Agronomy 11, 993. https://doi.org/10.3390/agronomy11050993.

de Almeida, S.G.C., Tarelho, L.A.C., Hauschild, T., Costa, M.A.M., Dussán, K.J., 2022. Biochar production from sugarcane biomass using slow pyrolysis: characterization of the solid fraction. Chem. Eng. Process - Process Intensif. 179, 109054. https://doi.org/10.1016/j.cep.2022.109054.

Arafat Hossain, M., Ganesan, P., Jewaratnam, J., Chinna, K., 2017. Optimization of process parameters for microwave pyrolysis of oil palm fiber (OPF) for hydrogen and biochar production. Energy Convers. Manag 133, 349–362. https://doi.org/10.1016/j.enconman.2016.10.046.

Assirey, E.A., Altamimi, L.R., 2021. Chemical analysis of corn cob-based biochar and its role as water decontaminants. J. Taibah Univ. Sci. 15, 111–121. https://doi.org/10.1080/16583655.2021.1876350.

Bayoka, H., Snoussi, Y., Bhakta, A.K., El Garah, M., Khalil, A.M., Jouini, M., et al., 2023. Evidencing the synergistic effects of carbonization temperature, surface composition and structural properties on the catalytic activity of biochar/bimetallic composite. J. Anal. Appl. Pyrolysis 173, 106069. https://doi.org/10.1016/j.jaap.2023.106069.

Biswas, B., Pandey, N., Bisht, Y., Singh, R., Kumar, J., Bhaskar, T., 2017. Pyrolysis of agricultural biomass residues: comparative study of corn cob, wheat straw, rice straw and rice husk. Bioresour. Technol. 237, 57–63. https://doi.org/10.1016/j.biortech.2017.02.046.

Bourke, J., Manley-Harris, M., Fushimi, C., Dowaki, K., Nunoura, T., Antal, M.J., 2007. Do all carbonized charcoals have the same chemical structure? 2. A model of the chemical structure of carbonized charcoal. Ind. Eng. Chem. Res. 46, 5954–5967. https://doi.org/10.1021/ie070415u.

Briones, M.J.I., 2014. Soil fauna and soil functions: a jigsaw puzzle. Front. Environ. Sci. 2. https://doi.org/10.3389/fenvs.2014.00007.

Chen, J., Fang, D., Duan, F., 2018. Pore characteristics and fractal properties of biochar obtained from the pyrolysis of coarse wood in a fluidized-bed reactor. Appl. Energy 218, 54–65. https://doi.org/10.1016/j.apenergy.2018.02.179.

David, E., 2022. Production of activated biochar derived from residual biomass for adsorption of volatile organic compounds. Materials 16, 389. https://doi.org/10.3390/ma16010389.

Değermenci, G.D., Değermenci, N., Ayvaoğlu, V., Durmaz, E., Çakır, D., Akan, E., 2019. Adsorption of reactive dyes on lignocellulosic waste; characterization, equilibrium, kinetic and thermodynamic studies. J. Clean. Prod. 225, 1220–1229. https://doi.org/10.1016/j.jclepro.2019.03.260.

Dhar, S.A., Sakib, T.U., Hilary, L.N., 2022. Effects of pyrolysis temperature on production and physicochemical characterization of biochar derived from coconut fiber biomass through slow pyrolysis process. Biomass-.-. Convers. Biorefinery 12, 2631–2647. https://doi.org/10.1007/s13399-020-01116-y.

Divyangkumar, N., Panwar, N.L., 2024. Standardization, certification, and development of biochar based fertilizer for sustainable agriculture: an overview. Environ. Pollut. Manag 1, 186–202. https://doi.org/10.1016/j.epm.2024.10.001.

Divyangkumar, N., Panwar, N.L., Agrawal, C., Gupta, T., Meena, G.L., Singh, M., 2024. Cradle-to-gate analyses of biochar produced from agricultural crop residues by vacuum pyrolysis. Clean. Energy 8, 1–15. https://doi.org/10.1093/ce/zkae069.

Domingues, R.R., Trugilho, P.F., Silva, C.A., Melo, I.C.N.A. de, Melo, L.C.A., Magriotis, Z. M., et al., 2017. Properties of biochar derived from wood and high-nutrient biomasses with the aim of agronomic and environmental benefits. PLoS One 12, e0176884. https://doi.org/10.1371/journal.pone.0176884.

Durango Padilla, E.R., Hansted, F.A.S., Luna, C.M.R., de Campos, C.I., Yamaji, F.M., 2024. Biochar derived from agricultural waste and its application as energy source in blast furnace. Renew. Energy 220, 119688. https://doi.org/10.1016/j.renene.2023.119688.

Egene, C.E., Van Poucke, R., Ok, Y.S., Meers, E., Tack, F.M.G., 2018. Impact of organic amendments (biochar, compost and peat) on Cd and Zn mobility and solubility in contaminated soil of the Campine region after three years. Sci. Total Environ. 626, 195–202. https://doi.org/10.1016/j.scitotenv.2018.01.054.

Eke, J., Onwudili, J.A., Bridgwater, A.V., 2020. Influence of moisture contents on the fast pyrolysis of trommel fines in a bubbling fluidized bed reactor. Waste Biomass-.-. Valoriz. 11, 3711–3722. https://doi.org/10.1007/s12649-018-00560-2.

El-Esawi M.A. Maize Genetic Resources - Breeding Strategies and Recent Advances 2021.

El-Sayed, S.A., Mostafa, M.E., 2015. Kinetic parameters determination of biomass pyrolysis fuels using TGA and DTA techniques. Waste Biomass-.-. Valoriz. 6, 401–415. https://doi.org/10.1007/s12649-015-9354-7.

Foong, S.Y., Liew, R.K., Yang, Y., Cheng, Y.W., Yek, P.N.Y., Wan Mahari, W.A., et al., 2020. Valorization of biomass waste to engineered activated biochar by microwave pyrolysis: progress, challenges, and future directions. Chem. Eng. J. 389, 124401. https://doi.org/10.1016/j.cej.2020.124401.

Gao, Y., Yue, Q., Gao, B., Sun, Y., Wang, W., Li, Q., et al., 2013. Preparation of high surface area-activated carbon from lignin of papermaking black liquor by KOH activation for Ni(II) adsorption. Chem. Eng. J. 217, 345–353. https://doi.org/10.1016/j.cej.2012.09.038.

Gęca, M., Khalil, A.M., Tang, M., Bhakta, A.K., Snoussi, Y., Nowicki, P., et al., 2023. Surface treatment of biochar—methods, surface analysis and potential applications: a comprehensive review. Surfaces 6, 179–213. https://doi.org/10.3390/surfaces6020013.

Gupta, G.K., Ram, M., Bala, R., Kapur, M., Mondal, M.K., 2018. Pyrolysis of chemically treated corncob for biochar production and its application in Cr(VI) removal. Environ. Prog. Sustain Energy 37, 1606–1617. https://doi.org/10.1002/ep.12838.

Huang, K., Li, M., Li, R., Rasul, F., Shahzad, S., Wu, C., et al., 2023. Soil acidification and salinity: the importance of biochar application to agricultural soils. Front Plant Sci. 14. https://doi.org/10.3389/fpls.2023.1206820.

Inyang, M., Gao, B., Pullammanappallil, P., Ding, W., Zimmerman, A.R., 2010. Biochar from anaerobically digested sugarcane bagasse. Bioresour. Technol. 101, 8868–8872. https://doi.org/10.1016/j.biortech.2010.06.088.

Jawad, A.H., Saud Abdulhameed, A., Wilson, L.D., Syed-Hassan, S.S.A., ALOthman, Z.A., Rizwan Khan, M., 2021. High surface area and mesoporous activated carbon from KOH-activated dragon fruit peels for methylene blue dye adsorption: optimization and mechanism study. Chin. J. Chem. Eng. 32, 281–290. https://doi.org/10.1016/j.cjche.2020.09.070.

Jindo, K., Mizumoto, H., Sawada, Y., Sanchez-Monedero, M.A., Sonoki, T., 2014. Physical and chemical characterization of biochars derived from different

agricultural residues. Biogeosciences 11, 6613–6621. https://doi.org/10.5194/bg-11-6613-2014.
Kalair, A.R., Seyedmahmoudian, M., Stojcevski, A., Abas, N., Khan, N., 2021. Waste to energy conversion for a sustainable future. Heliyon 7, e08155. https://doi.org/10.1016/j.heliyon.2021.e08155.
Khalil, A.M., Michely, L., Pires, R., Bastide, S., Jlassi, K., Ammar, S., et al., 2021. Copper/nickel-decorated olive pit biochar: one pot solid state synthesis for environmental remediation. Appl. Sci. 11, 8513. https://doi.org/10.3390/app11188513.
Kolawole, I.D., Kolawole, G.O., Sanni-manuel, B.A., Kolawole, S.K., Ewansiha, J.U., Kolawole, V.A., et al., 2024. Economic impact of waste from food, water, and agriculture in Nigeria: challenges, implications, and applications—a review. Discov. Environ. 2, 51. https://doi.org/10.1007/s44274-024-00086-6.
Lanjekar, P.R., Panwar, N.L., Patel, M.R., Divyangkumar, N., 2024. Exploring sustainable energy: an overview of biochemical and thermochemical conversion of dairy and food waste. Environ. Pollut. Manag 1, 152–166. https://doi.org/10.1016/j.epm.2024.09.003.
Lei, O., Zhang, R., 2013. Effects of biochars derived from different feedstocks and pyrolysis temperatures on soil physical and hydraulic properties. J. Soils Sediment. 13, 1561–1572. https://doi.org/10.1007/s11368-013-0738-7.
Liang, B., Lehmann, J., Solomon, D., Kinyangi, J., Grossman, J., O'Neill, B., et al., 2006. Black carbon increases cation exchange capacity in soils. Soil Sci. Soc. Am. J. 70, 1719–1730. https://doi.org/10.2136/sssaj2005.0383.
Liew, R.K., Azwar, E., Yek, P.N.Y., Lim, X.Y., Cheng, C.K., Ng, J.-H., et al., 2018. Microwave pyrolysis with KOH/NaOH mixture activation: a new approach to produce micro-mesoporous activated carbon for textile dye adsorption. Bioresour. Technol. 266, 1–10. https://doi.org/10.1016/j.biortech.2018.06.051.
Liu, X., Mao, P., Li, L., Ma, J., 2019. Impact of biochar application on yield-scaled greenhouse gas intensity: a meta-analysis. Sci. Total Environ. 656, 969–976. https://doi.org/10.1016/j.scitotenv.2018.11.396.
Liu, Z., Dugan, B., Masiello, C.A., Gonnermann, H.M., 2017. Biochar particle size, shape, and porosity act together to influence soil water properties. PLoS One 12, e0179079. https://doi.org/10.1371/journal.pone.0179079.
Mishra, P., Al Khatib, A.M.G., Sardar, I., Mohammed, J., Karakaya, K., Dash, A., et al., 2021. Modeling and forecasting of sugarcane production in India. Sugar Tech. 23, 1317–1324. https://doi.org/10.1007/s12355-021-01004-3.
Mohan, D., Abhishek, K., Sarswat, A., Patel, M., Singh, P., Pittman, C.U., 2018. Biochar production and applications in soil fertility and carbon sequestration – a sustainable solution to crop-residue burning in India. RSC Adv. 8, 508–520. https://doi.org/10.1039/C7RA10353K.
Montero, J.I.Z., Monteiro, A.S.C., Gontijo, E.S.J., Bueno, C.C., de Moraes, M.A., Rosa, A.H., 2018. High efficiency removal of As(III) from waters using a new and friendly adsorbent based on sugarcane bagasse and corncob husk Fe-coated biochars. Ecotoxicol. Environ. Saf. 162, 616–624. https://doi.org/10.1016/j.ecoenv.2018.07.042.
Mubarak, N.M., Yusof, F., Alkhatib, M.F., 2011. The production of carbon nanotubes using two-stage chemical vapor deposition and their potential use in protein purification. Chem. Eng. J. 168, 461–469. https://doi.org/10.1016/j.cej.2011.01.045.
Mujtaba, G., Hayat, R., Hussain, Q., Ahmed, M., 2021. Physio-chemical characterization of biochar, compost and co-composted biochar derived from green waste. Sustainability 13, 4628. https://doi.org/10.3390/su13094628.
Nair, V.D., Nair, P.K.R., Dari, B., Freitas, A.M., Chatterjee, N., Pinheiro, F.M., 2017. Biochar in the agroecosystem–climate-change–sustainability Nexus. Front Plant Sci. 8. https://doi.org/10.3389/fpls.2017.02051.
Nam, W.L., Phang, X.Y., Su, M.H., Liew, R.K., Ma, N.L., Rosli, M.H.N.Bin, et al., 2018. Production of bio-fertilizer from microwave vacuum pyrolysis of palm kernel shell for cultivation of Oyster mushroom (Pleurotus ostreatus). Sci. Total Environ. 624, 9–16. https://doi.org/10.1016/j.scitotenv.2017.12.108.
Nazir, M.H., Ayoub, M., Zahid, I., Shamsuddin, R.B., Zulqarnain, Ameen, M., et al., 2022. Waste sugarcane bagasse-derived nanocatalyst for microwave-assisted transesterification: thermal, kinetic and optimization study. Biofuels, Bioprod. Bioref. 16, 122–141. https://doi.org/10.1002/bbb.2264.
Nhuchhen, D.R., Abdul Salam, P., 2012. Estimation of higher heating value of biomass from proximate analysis: a new approach. Fuel 99, 55–63. https://doi.org/10.1016/j.fuel.2012.04.015.
Padilla, E., Nakashima, G., Larissa, A., Hansted, S., Santos, L., Barros, J., et al., 2019. Thermogravimetric and ftir analyzes of corn cob pyrolysis. Quim. Nova 566–569. https://doi.org/10.21577/0100-4042.20170360.
Patel, M.R., Panwar, N.L., 2024. Development, process optimization and assessment of sustainable mobile biochar kiln for agricultural use. J. Clean. Prod. 477, 143866. https://doi.org/10.1016/j.jclepro.2024.143866.
Pinky, N.S., Bin Mobarak, M., Mustafi, S., Zesanur Rahman, M., Nahar, A., Saha, T., et al., 2023. Facile preparation of micro-porous biochar from Bangladeshi sprouted agricultural waste (corncob) via in-house built heating chamber for cationic dye removal. Arab J. Chem. 16, 105080. https://doi.org/10.1016/j.arabjc.2023.105080.
Qian, C., Li, Q., Zhang, Z., Wang, X., Hu, J., Cao, W., 2020. Prediction of higher heating values of biochar from proximate and ultimate analysis. Fuel 265, 116925. https://doi.org/10.1016/j.fuel.2019.116925.
Qiu, Q., Zhou, M., Cai, W., Zhou, Q., Zhang, Y., Wang, W., et al., 2019. A comparative investigation on direct carbon solid oxide fuel cells operated with fuels of biochar derived from wheat straw, corncob, and bagasse. Biomass-.-. Bioenergy 121, 56–63. https://doi.org/10.1016/j.biombioe.2018.12.016.
Ronsse, F., van Hecke, S., Dickinson, D., Prins, W., 2013. Production and characterization of slow pyrolysis biochar: influence of feedstock type and pyrolysis conditions. GCB Bioenergy 5, 104–115. https://doi.org/10.1111/gcbb.12018.
Roy, S., Kumar, U., Bhattacharyya, P., 2019. Synthesis and characterization of exfoliated biochar from four agricultural feedstock. Environ. Sci. Pollut. Res 26, 7272–7276. https://doi.org/10.1007/s11356-018-04117-7.
Siddiqui, M.T.H., Nizamuddin, S., Mubarak, N.M., Shirin, K., Aijaz, M., Hussain, M., et al., 2019. Characterization and process optimization of biochar produced using novel biomass, waste pomegranate peel: a response surface methodology approach. Waste Biomass-.-. Valoriz. 10, 521–532. https://doi.org/10.1007/s12649-017-0091-y.
Smith, S.C., Rodrigues, D.F., 2015. Carbon-based nanomaterials for removal of chemical and biological contaminants from water: a review of mechanisms and applications. Carbon N. Y 91, 122–143. https://doi.org/10.1016/j.carbon.2015.04.043.
Sohaib, Q., Muhammad, A., Younas, M., 2017. Fast pyrolysis of sugarcane bagasse: effect of pyrolysis conditions on final product distribution and properties. Energy Sources, Part A Recover Util. Environ. Eff. 39, 184–190. https://doi.org/10.1080/15567036.2016.1212292.
Stylianou, M., Christou, A., Dalias, P., Polycarpou, P., Michael, C., Agapiou, A., et al., 2020. Physicochemical and structural characterization of biochar derived from the pyrolysis of biosolids, cattle manure and spent coffee grounds. J. Energy Inst. 93, 2063–2073. https://doi.org/10.1016/j.joei.2020.05.002.
Sun, J., He, F., Pan, Y., Zhang, Z., 2017. Effects of pyrolysis temperature and residence time on physicochemical properties of different biochar types. Acta Agric. Scand. Sect. B — Soil Plant Sci. 67, 12–22. https://doi.org/10.1080/09064710.2016.1214745.
Tehreem, S., Yousra, M., Alamer, K.H., Alsudays, I.M., Sarwar, S., Kamal, A., et al., 2022. Analysis of the role of various biochar in the remediation of heavy metals in contaminated water and its kinetics study. J. Saudi Chem. Soc. 26, 101518. https://doi.org/10.1016/j.jscs.2022.101518.
Tomczyk, A., Sokołowska, Z., Boguta, P., 2020. Biochar physicochemical properties: pyrolysis temperature and feedstock kind effects. Rev. Environ. Sci. Bio/Technol. 19, 191–215. https://doi.org/10.1007/s11157-020-09523-3.
Toscano Miranda, N., Lopes Motta, I., Maciel Filho, R., Wolf Maciel, M.R., 2021. Sugarcane bagasse pyrolysis: a review of operating conditions and products properties. Renew. Sustain Energy Rev. 149, 111394. https://doi.org/10.1016/j.rser.2021.111394.
Uras, Ü., Carrier, M., Hardie, A.G., Knoetze, J.H., 2012. Physico-chemical characterization of biochars from vacuum pyrolysis of South African agricultural wastes for application as soil amendments. J. Anal. Appl. Pyrolysis 98, 207–213. https://doi.org/10.1016/j.jaap.2012.08.007.
V, K.K., Panwar, N.L., 2024. Pyrolysis technologies for biochar production in waste management: a review. Clean. Energy 8, 61–78. https://doi.org/10.1093/ce/zkae036.
Wang, B., Gao, B., Fang, J., 2017. Recent advances in engineered biochar productions and applications. Crit. Rev. Environ. Sci. Technol. 47, 2158–2207. https://doi.org/10.1080/10643389.2017.1418580.
Wang, X., Cheng, H., Ye, G., Fan, J., Yao, F., Wang, Y., et al., 2022. Key factors and primary modification methods of activated carbon and their application in adsorption of carbon-based gases: a review. Chemosphere 287, 131995. https://doi.org/10.1016/j.chemosphere.2021.131995.
Zhang, C., Liu, L., Zhao, M., Rong, H., Xu, Y., 2018. The environmental characteristics and applications of biochar. Environ. Sci. Pollut. Res. 25, 21525–21534. https://doi.org/10.1007/s11356-018-2521-1.